JOURNAL OF APPLIED ELECTROCHEMISTRY 4 (1974) 135–142

Electrochemical capacitance characterization of n-type gallium arsenide

T. AMBRIDGE and M. M. FAKTOR

Post Office Research Department, Dollis Hill, London

Received 1st October 1973

The depletion layer capacitance of n-type gallium arsenide was measured as a function of its anodic potential in an electrochemical cell. It was shown that these measurements can lead to accurate values of carrier concentration, and are compatible with stripping by electrochemical dissolution, provided that surface area is preserved. The experimental conditions required to maintain the electrolyte-semiconductor contact area constant, are described. Also, it is shown that excursions into regions outside those specified lead to significant enhancement of capacity (via real area increase). Under these conditions the carrier concentration can no longer be obtained but much can be learnt about the internal structure of the material.

1. Introduction

The electrochemical behaviour of the interface between a semiconductor electrode and an electrolyte depends, under certain conditions, upon the conductivity and doping type of the semiconductor [1, 2, 3]. In particular, under anodic polarization, the interface between an n-type semiconductor and a concentrated electrolyte can be considered as a Schottky barrier, which determines both electrical behaviour [4, 5] and dissolution rate [4], within a limited range of applied potentials. Current-voltage [4] and capacitance-voltage [5] measurements have been used to estimate values of carrier concentration, with the latter method yielding the best quantitative results to date. Electrochemical etching reveals features which can be correlated with defects in the material [4, 6, 7], with the relative enhancement of different defects depending on the precise conditions of anodic dissolution.

In the present work we have studied the electrochemical capacitance-voltage behaviour of gallium arsenide (with doping levels between 10^{16} and greater than 10^{18} cm^{-3}) as a function of dissolution conditions, which are varied by the absence or presence of illumination. Two distinctly different etching regimes have been distinguished. In one a gross enhancement of surface area is indicated by visual examination, and confirmed by capacitance measurements. Increases by factors of up to 7 have been observed. In the other etching regime, the increase in capacitance is negligible following extensive dissolution, and accurate values of carrier concentration may be deduced, which are in close agreement with Hall measurements. It is thus demonstrated that by operating in the 'safe' regime a carrier concentration depth profile, with essentially no depth limit, may readily be obtained, while additional information on defects may be forthcoming from separate studies of areas etched in the other regime. In addition, a correlation between doping inhomogeneities in material, indicated by electrochemical capacitance measurements, and features revealed by dissolution, is described.

2. Experimental

2.1 *Apparatus*

The electrolytic cell has previously been described [4]. Briefly it consisted of a simple arrangement whereby a well-defined area of one face of a GaAs slice was held in contact with flowing aqueous KOH solution with provision for illumination of the interface via an integral light-pipe. Two back contacts were provided to the slice: Potential measurements were made via one of these contacts with respect to a saturated calomel electrode (SCE) in contact with the electrolyte, while current was passed between the other contact, and a carbon working electrode. Automatic current voltage characteristic plotting was employed as used previously [8]. For the present work, an A.C. coupled autobalance capacitance bridge, Wayne Kerr type B641, operating at 1·592 KHz, and a voltage sweep unit, Hewlett Packard function generator type 3310B, were connected in parallel between the 'current' contact and the carbon electrode. The latter unit was connected via a 100 H series inductance to provide effective isolation at the operating frequency of the bridge, and a triangular sweep function of 0·015 Hz frequency was employed. Capacitance-voltage curves were plotted on an *x-y* recorder.

Several simple modifications to the basic cell system have also been made since the earlier published work [4]. The O-ring used to define the area of sample in contact with the electrolyte was replaced by a short, 4 mm diameter, thin-walled ceramic tube with a silicone rubber coating, resulting in highly reproducible area definition. Secondly, improved back contacts have been obtained by coating the gold probes with tin (a donor in gallium arsenide) yielding, upon forming, contact resistances of between 1 Ω and 6 Ω, depending upon the doping level of the gallium arsenide. Finally, an improved light guiding system has been incorporated, which, in conjunction with a 250 W quartz iodine tungsten light source has permitted the attainment of much higher illumination levels than used previously.

2. *Procedure*

Six different samples of gallium arsenide single crystals, sliced on the (100) plane from boat grown or Czochralski grown ingots, were selected. These included commercial-grade material supplied by Bell and Howell Inc. (U.S.A.), and Mining and Chemical Products (U.K.), and, also, an example of dislocation-free material grown at the Battelle Memorial Institute [9, 10], as listed in Table 1. The front faces were mechano-chemically polished using bromine in methanol [11], and followed by chemical polishing in H_2SO_4:H_2O_2:H_2O (3:1:1) just prior to the measurement. Current-voltage characteristics were measured on test areas of each material,

Table 1

Sample	*Supplier*	*Ingot No.*	*Dopant*	*Test area*	*Carrier concentration* (Hall) *electrons cm*$^{-3}$	*Carrier concentration (electrochemical capacitance) electrons cm*$^{-3}$	*Stripping mode*	n/n_0	A/A_0
A	MCP	X2544	Si	I	$2{\cdot}57\times10^{18}$	$2{\cdot}27\times10^{18}$	Illuminated	1·08	1·04
				II	—	$2{\cdot}24\times10^{18}$	Dark	8·74	2·96
				III	$1{\cdot}63\times10^{18}$	$1{\cdot}46\times10^{18}$	Illuminated	1·07	1·03
B	Battelle		Si	I	$1{\cdot}32\times10^{18}$	$1{\cdot}26\times10^{18}$	Illuminated	1·03	1·01
				II	—	$1{\cdot}25\times10^{18}$	Dark	43·9	6·63
C	B&H		Si	I	$4{\cdot}12\times10^{17}$	$4{\cdot}17\times10^{17}$	Illuminated	1·09	1·04
D	MCP	AX656A	Sn	I	$1{\cdot}48\times10^{17}$	$1{\cdot}46\times10^{17}$	Illuminated	1·07	1·03
E	B&H		None	I	$3{\cdot}75\times10^{16}$	$5{\cdot}11\times10^{16}$	Illuminated	1·08	1·04
				II	$3{\cdot}67\times10^{16}$	$4{\cdot}69\times10^{16}$	Illuminated	1·08	1·04
				III	$3{\cdot}45\times10^{16}$	$6{\cdot}25\times10^{16}$	Illuminated	1·27	1·13
				IV	—	$5{\cdot}70\times10^{16}$	Dark	32·9	5·73
F	MCP	A1082	None	I	$3{\cdot}34\times10^{16}$	$6{\cdot}67\times10^{16}$	Illuminated	0·94	0·97

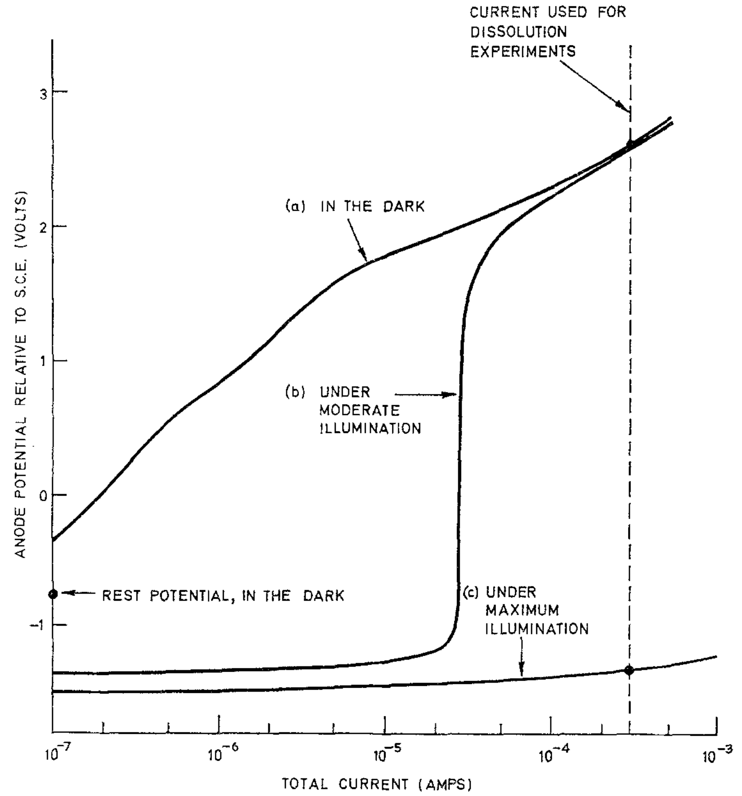

Fig. 1. Voltage versus log current characteristics for the medium-doped n-type GaAs sample C (see Table 1): (a) in the dark, (b) under 'band-gap' illumination using a tungsten source and a narrowband optical filter, and (c) under intense tungsten illumination (for which the saturation photocurrent region was not reached). The rest potential is marked.

both in the dark and at different illumination levels, in a manner similar to that reported earlier [4, 8]. Typical curves (for the medium-doped specimen C) are shown in Fig. 1, plotted in the form of voltage versus log current. It has been established that, at sufficiently low potentials, the observed current under illumination is determined by holes generated in the near surface region of the gallium arsenide, so that the anodic dissolution rate is controlled by the light intensity [4]. It should be noted that there is a potential region in which a saturation current is approached, its value being proportional to light intensity. At sufficiently high potentials, a current is also observed in the dark, as shown. No detailed explanation for this current has yet been proposed, since it is observed at much lower voltages than those normally associated with avalanche breakdown in material with the same average doping level [12].

Because early experiments had shown that deep pitting can occur when dissolution takes place via the anomalous dark current mechanism, initial dark capacitance-voltage measurements were performed on fresh areas of each sample, using a restricted voltage sweep, to ensure that negligible dissolution occurred while tracing a curve. In practice this meant that the maximum anodic potential was chosen to correspond to a current density of less than 10^{-7} A cm^{-2} (so that less than 1 Å was removed per plotting cycle), whilst the minimum potential was fixed just above the rest potential. Fig. 2 shows a plot taken for the sample represented in Fig. 1. (Note that voltage is shown as the ordinate, to correlate with the voltage-log current plots.)

Following these initial capacitance measurements, material was removed in stages by anodic dissolution, either under intense tungsten filament

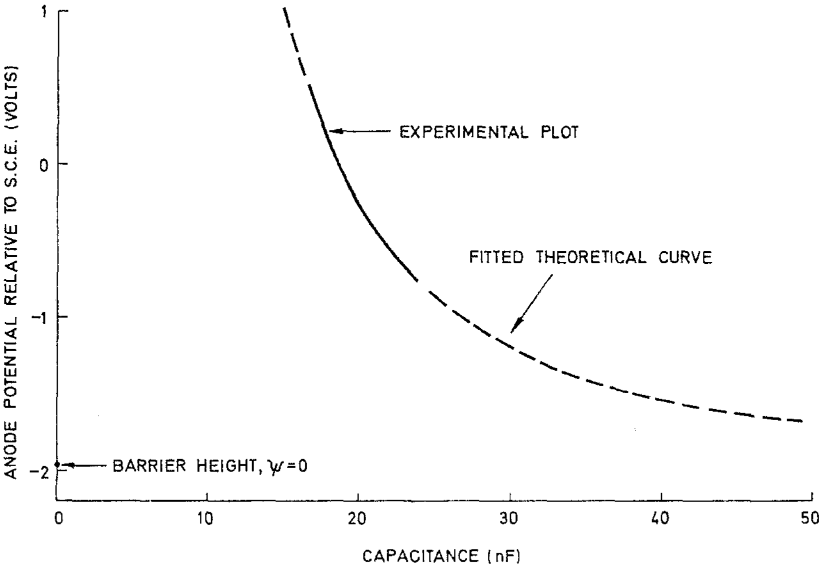

Fig. 2. Voltage versus electrochemical capacitance for sample C, showing a theoretica curve exactly super-imposed on the experimental plot. Also shown is the point on the potential axis which corresponds to zero potential barrier height, as deduced from the curve fitting.

illumination, or in the dark, but in both cases fixing the dissolution current at a value of 3×10^{-4} A, as indicated by the markers on Fig. 1. The amount of material removed at each stage was estimated from the measured total charge transfer (integrated current), on the assumption that six units of charge were involved in the reaction for the dissolution of one molecular weight unit of gallium arsenide [13]. Further capacitance measurements were made at each stripping stage. The total amount of material removed from each sample corresponded to an 'equivalent' depth of 10 μm removed, on the assumption of uniform stripping over the entire exposed area; the limitations of this assumption in different circumstances will become apparent. The removal rate was equivalent to approximately 0·1 μm min^{-1}.

Visual examination was carried out subsequently, followed in some cases by optical microscopy, scanning electron microscopy, and surface roughness measurements using a Rank-Taylor-Hobson 'Talysurf' instrument. Those samples which were etched under illumination, and had hence not suffered gross topographical disturbances, were then subjected to Hall effect measurements of carrier concentration. For this purpose, a 2·5 mm diameter disc was taken from the centre of each etched area by ultrasonic drilling, and these were further etched in H_2SO_4:H_2O_2:H_2O (3:1:1) to remove work damage before the measurements were taken using a Van der Pauw [14] four probe arrangement.

3. Results

Table 1 lists, in decreasing order of carrier concentration, the samples studied; at each end of the carrier concentration range, electrochemical measurements were made on different areas of the same sample, while samples of intermediate doping level were examined less extensively. In each case, the initial carrier concentration is given, as indicated by electrochemical capacitance measurements in the dark. These were obtained by matching the experimental curves to theoretical curves derived from the Schottky barrier formula [15], for depletion layer capacitance:

$$C = \left[\frac{qn\varepsilon_0\varepsilon}{2}\right]^{\frac{1}{2}} \psi^{-\frac{1}{2}} A$$

where q = electronic charge, n = net donor concentration, ε_0 = absolute permittivity of free space, ε = relative permittivity of gallium arsenide, ψ = potential barrier height and A = area exposed to electrolyte.

The values obtained are plotted in Fig. 3 against those obtained from the Hall effect measurements (except for samples subsequently dissolved in the dark).

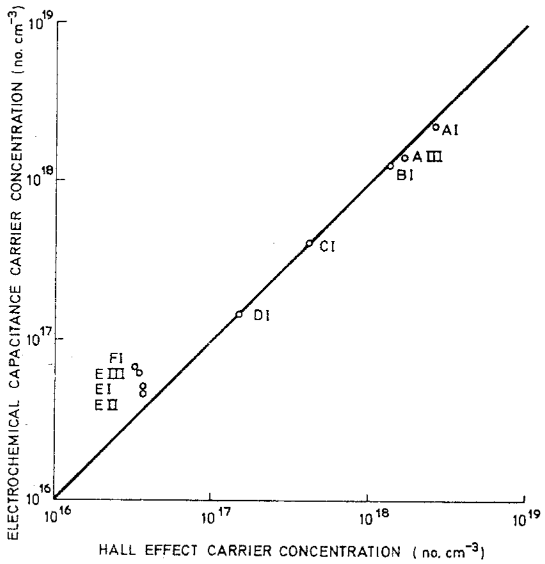

Fig. 3. Carrier concentration, determined from electrochemical capacitance, versus carrier concentration given by the Hall effect, for samples listed in Table 1.

The final columns in the table indicate the apparent increase in carrier concentration (n/n_0) following the removal of the equivalent of 10 μm of material, and, alternatively, the increase in effective surface area in contact with electrolyte (A/A_0) which is implied if it is assumed that the carrier concentration in fact remained unchanged. Note that the largest increases correspond to the three examples of dissolution in the dark. This is shown in more detail in Figs. 4 and 5, in which the increases are plotted as a function of the amount of material removed.

The final appearance of the above areas, dissolved in the dark is compared in Figs. 6, 7, and 8 with that of adjacent areas of the same samples stripped under illumination-controlled conditions. Where illumination was used, two concentric regions are apparent. The inner area, defined by the inner diameter of the coated ceramic tube, represents the dissolved illuminated area, while the existence of an outer rim suggests that electrolyte spread to the outer diameter of the tube. This is confirmed by the absence of an inner ring in the photographs of areas dissolved entirely in the dark, where the outer ring is just visible in Fig. 6b and clearly visible in Fig. 8b. (Occasional measurements in

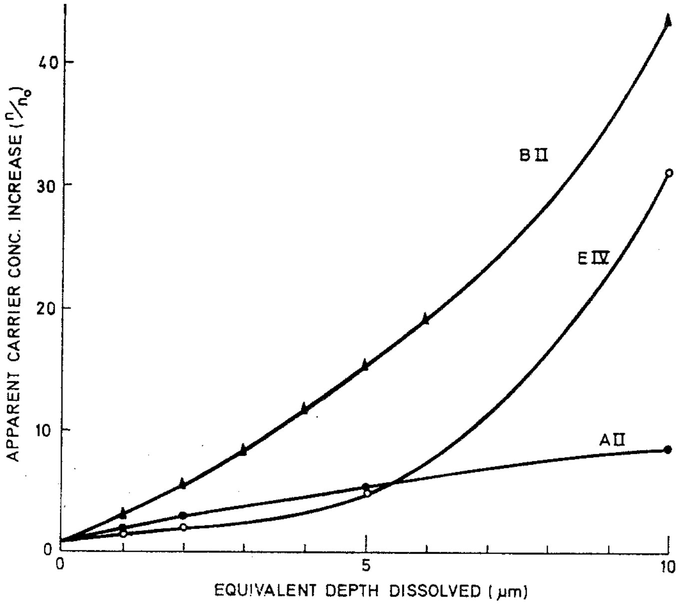

Fig. 4. The apparent increase in carrier concentration as a function of the amount of material removed (expressed as the equivalent average depth) by electrochemical dissolution in the dark, assuming no change in area. Refer to Table 1 for sample identification.

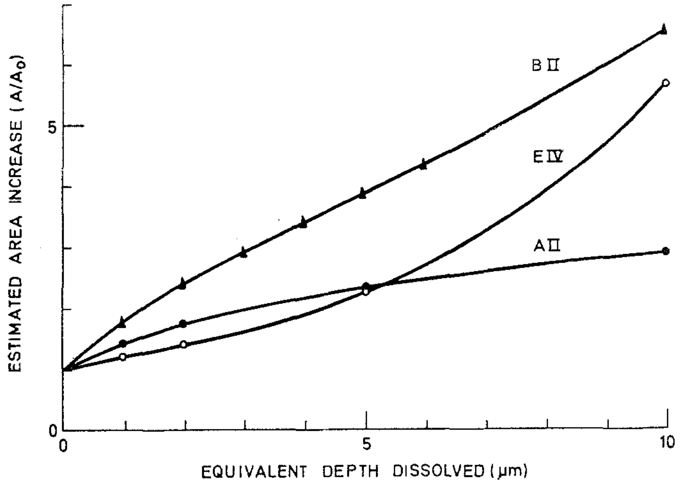

Fig. 5. The increase in effective surface area as a function of the amount of material removed, by dissolution in the dark, assuming no change in carrier concentration, for those samples depicted in Fig. 4.

the presence of illumination were made at stages during the dark dissolution of the sample shown in Fig. 7b; hence the inner ring.) The two different areas were taken into account (a) in determining the depth corresponding to the amount of material removed during 'uniform' stripping under illumination, and (b) in deducing carrier concentration from the dark capacitance.

Variations in etching characteristics between different areas of the same slice were also observed, under identical dissolution conditions. Fig. 9a shows the whole of the most highly doped sample A, upon which five different areas were examined, including the two depicted in Fig. 8. The striations, which are clearly visible in areas either side of the central region, were faintly visible following the initial etch/polish. Area III shown in Fig. 9b (from the lower centre of Fig. 9a) is to be compared with area I shown in Fig. 8a; both were stripped under illumination. The corresponding carrier concentration measurements (from the Table) showed an average value 50% higher in the heavily striated region than in the relatively smooth region.

Microscopic details of the topography of etched areas are the subject of a separate paper [7]. Examples are shown, however, in Fig. 10, of scanning electron micrographs of one of the isolated, deep pits apparent after the dark dissolution of area IV of the heavily doped sample A (Fig. 9a). A 'Talysurf' trace across the two major channels formed in area II, apparently by the coalescence of similar pits along striation lines, is shown in Fig. 11. The volume of these channels accounted for 75% of the total material removed from the exposed area. Examples of roughness traces across the surfaces remaining after dissolution of specimens under illumination, are shown in Fig. 12.

4. Discussion

The close agreement between values of carrier concentration measured by the electrochemical capacitance method and those obtained from Hall measurements confirms the reliability of the method. There is, however, a discrepancy apparent for the material with the lowest carrier concentration; the capacitance method suggests larger values. The most likely explanation for this is that this method includes a contribution from deep levels, whose concentration is in this case large compared with that of the shallow levels which determine the carrier concentration. The use of a higher frequency (e.g. 1 MHz) for the capacitance measurements would then eliminate this contribution; alternatively a more detailed frequency-dependent analysis should yield quantitative information on deep and shallow levels [16, 17]. This is supported by the fact that some hysteresis was apparent in our capacitance measurements for the low-doped

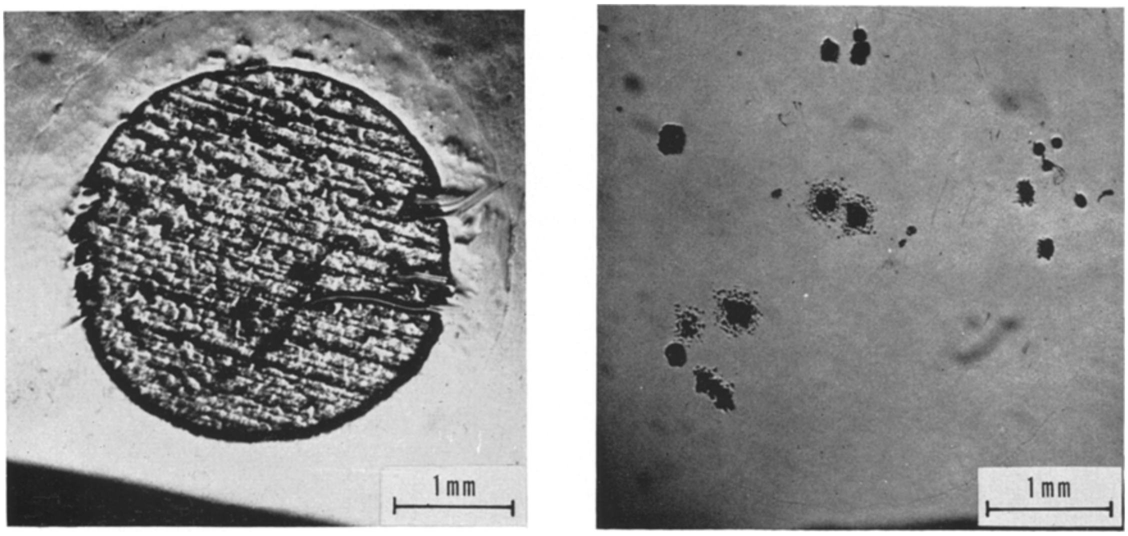

(a) (b)

Fig. 6. Comparison of areas after removal of 10 μm (equivalent) of material by dissolution (a) under illumination, and (b) in the dark, showing areas III and IV respectively of sample E (low doped).

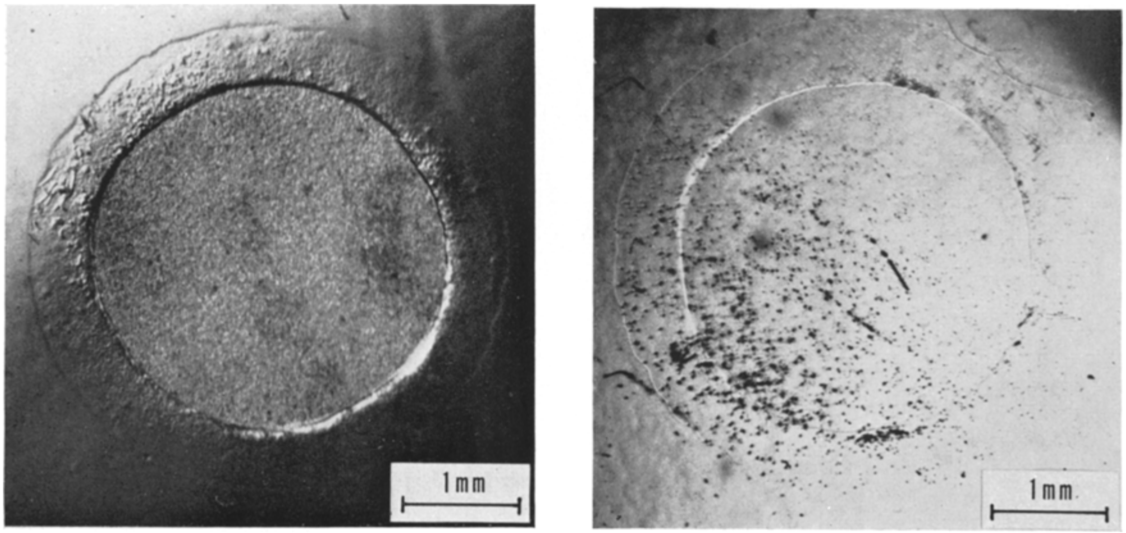

(a) (b)

Fig. 7. As for Fig. 6, showing areas I and II of sample B (highly doped, dislocation free). Note that area II was briefly illuminated during dissolution which was otherwise in the dark.

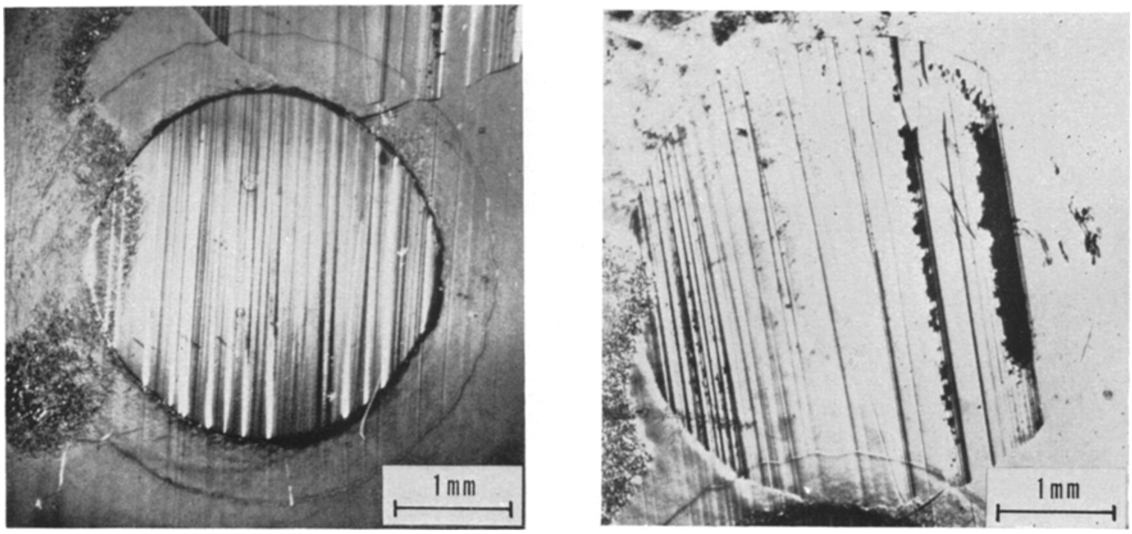

(a) (b)

Fig. 8. As for Fig. 6, showing areas I and II of sample A (highly doped).

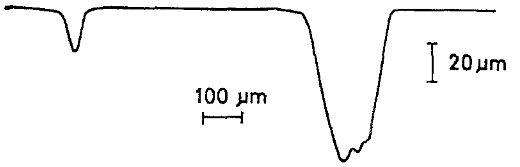

Fig. 11. The depths of the two major channels formed by dark dissolution of sample A, area II (Fig. 8b), shown on a 'Talysurf' trace perpendicular to the direction of the striations.

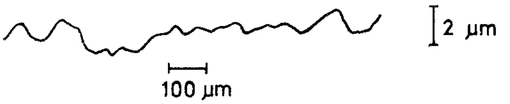

(a) E III

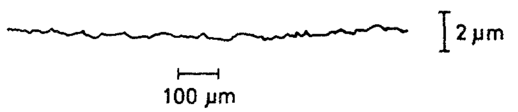

(b) B I

Fig. 12. Topography of the surfaces of (a) sample E, area III (low doped), and (b) sample B, area I (highly doped, dislocation free) following the removal of 10 μm of material by dissolution under illumination. 'Talysurf' trace 'a' was taken perpendicular to the direction of the striations.

samples, and that a frequency-dependence in a similar system has been reported by Birintseva and Pleskov [18]. A possibility that cannot be overlooked is that interfacial states contribute to the effect. Further studies are planned to clarify these points, but the present results demonstrate in principle the potential usefulness of this technique.

It is clear that, when dissolution is used in conjunction with capacitance measurements, as for example in the determination of carrier concentration depth profiles, preservation of area is essential, and that this is achieved quite well by stripping under illumination controlled conditions. Despite the roughness of the final surfaces clearly shown in the photographs, the increase in area, following the removal of 10 μm, was only 3–4% for typical material, as indicated by capacitance measurements, leading to an error in carrier concentration of 7–8%, if not taken into account. Since an allowance could be made the error becomes insignificant for most purposes. Less than 1% increase in area is expected from the side wall of the etched area. Analysis of the 'Talysurf' measurements suggests that the visible roughness accounts for very little of the remaining area increase (less than 0·1% enhancement), since the scale of variations normal to the surface is much smaller than that of variations parallel to the surface; hence changes on a much finer, lateral scale may be responsible. The geometric nature of the undulations, the correlation of striated regions with increased doping level in one sample, and the relative uniformity of attack on dislocation-free material, all confirm that material inhomogeneities of one form or another play an important role. In particular, striation ridges, occurring during photo-etching of n-type gallium arsenide have been reported by Kuhn-Kuhnenfeld [6] as zones of higher carrier concentration. The same conclusion would follow from our earlier work [4], which showed that dissolution rates are slower where carrier concentration is higher (or minority carrier lifetime smaller), under similar potential and illumination conditions. Thus, although our measurements showed 50% higher average carrier concentration in the regions of the high-doped specimen in which striations appeared, the maximum carrier concentration, corresponding to the ridges themselves, would have been even higher, indicating quite gross inhomogeneity of doping.

The results of dissolution in the dark are of interest for several reasons. First, the capacitance measurements show that it is essential to avoid this stripping regime if accurate evaluation of carrier concentration is required. The effect of area enhancement results in grossly exaggerated estimates of carrier concentration, as is obvious from Figs. 4 and 5, because of the square law dependence on capacitance. Secondly, the combination of capacitance measurements with topographical studies of the attacked regions provides more clues as to their nature. Scanning electron microscopy shows that the features revealed by dissolution in the dark take the form of deep pits, usually containing stacks of fibres which have apparently resulted from the collapse of the initial walls of the pits. The increased capacitance indicates that the total surface areas of all such regions can be many times greater than the initial geometric area of exposed surface, confirming a quite remarkable degree of structure within the pits. In addition, the facts that the Schottky barrier law was well obeyed, and that no gross changes in contact potential (barrier height for zero current) occurred throughout the dissolution, are evidence that the surfaces revealed retain the characteristics of gallium arsenide material, and are not, for example, significantly decorated with some impurity. It remains possible that some of the increased capacitance could be due to a higher carrier concentration in the regions where pitting occurs. Since these regions are confined to small areas of the original surface, such an effect could help to explain why anomalously high dark currents can be drawn. The dark current is clearly associated with these regions, as it is only here that significant dissolution occurs in the dark, and current-voltage measurements show that this current increases, at a given potential, as the pits develop. High field induced breakdown would be expected to occur in regions of higher carrier concentration at lower voltages than those associated with breakdown in the rest of the material. Although these regions would contribute little to the initially measured carrier concentration, their contribution would increase as the surface area of the pits increased. A closer investigation of this problem would benefit from an independent method of determining surface area enhancement, and a detailed study of the current-voltage behaviour. However it must not be overlooked that the role of crystalline defects, and not simply inhomogeneities of doping, have to be considered in the overall picture, although this aspect is beyond the scope of this paper. The topic is pursued in a another publication [7] in which more emphasis is placed on the topographical nature of the features revealed, and further evidence is presented.

5. Conclusion

It has been shown that electrochemical capacitance voltage measurements can be used to determine accurate values of carrier concentration of gallium arsenide specimens, and that controlled dissolution under illumination permits measurements to be made at any required depth beneath the original surface. Capacitance measurements are shown to provide a useful tool in the investigation of features revealed by different modes of electrochemical etching.

Acknowledgements

Acknowledgement is made to our colleagues M. R. Taylor, D. G. Fiddyment and E. Bremner, both for useful discussions and contributions to the experimental work, and to the Director of Research of the Post Office for permission to publish this paper.

References

[1] V. A. Myamlin and Yu V. Pleskov, *Electrochemistry of Semiconductors*, Plenum Press, New York (1967).

[2] P. J. Boddy, *Progress in Solid State Chemistry* Vol. 4, Ed. H. Reiss, Pergamon Press, Oxford (1967).

[3] H. Gerischer, *Physical Chemistry—An Advanced Treatise: IXa Electrochemistry*, Ch. 5, Ed. H. Eyring, J. Henderson and W. Jost, Academic Press, New York (1970).

[4] T. Ambridge, C. R. Elliott and M. M. Faktor, *J. Appl. Electrochem.* **3** (1973) 1.

[5] A. Yamashita, H. Araki and T. Aoki, *Jap. J. Appl. Phys.* **11** (1972) 908.

[6] F. Kuhn-Kuhnenfeld, *J. Electrochem. Soc.* **119** (1972), 1064.

[7] D. G. Fiddyment, M. R. Taylor and M. M. Faktor, to be published.

[8] E. G. Bremner, T. Ambridge and C. R. Elliott, *J. Phys. E: Sci. Instrum.* **6** (1973) 326.

[9] A. Steinemann and U. Zimmerli, *Solid State Electronics* **6** (1963) 597.

[10] A. Steinemann and U. Zimmerli, Proc. Internat. Conf. on Crystal Growth Boston 20–14 June 19-6, in 'Crystal Growth' (Suppl. to *J. Phys. Chem. Sol.*) Pergamon Press, Oxford (1967) 81.

[11] M. V. Sullivan and G. V. Kolb, *J. Electrochem. Soc.* **110** (1963) 585.

[12] S. M. Sze and G. Gibbons, *Appl. Phys. Lett.* **8** (1966) 111.

[13] H. Gerischer, *Ber. Bunsengessell. Phys. Chem.* **69** (1965) 578.

[14] L. J. Van der Pauw, *Philips Res. Repts.* **13** (1958) 1.

[15] A. Van der Ziel, *Solid State Physical Electronics* 2nd edition, p. 267, Prentice-Hall, New Jersey (1968).

[16] M. Bleicher and E. Lange, *Solid State Electronics* **16** (1973) 375.

[17] Y. Zohta, *Solid State Electronics* **16** (1973) 1029.

[18] T. P. Birintseva and Yu V. Pleskov, *Bull. Acad. Sciences (USSR)—Chem.*, **2** (1965) 236.

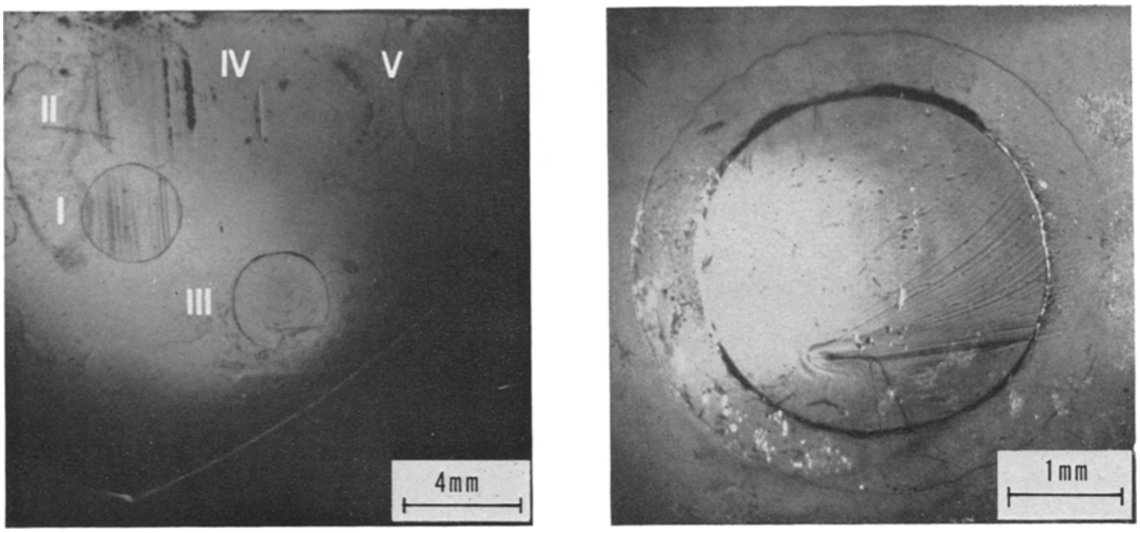

(a) (b)

Fig. 9. Inhomogeneity of sample A demonstrated (a) by an overall view of the slice, showing variations in the density of striations developed by electrochemical dissolution, and (b) by a view of area III which contrasts with area I (Fig. 8a) obtained under identical dissolution conditions.

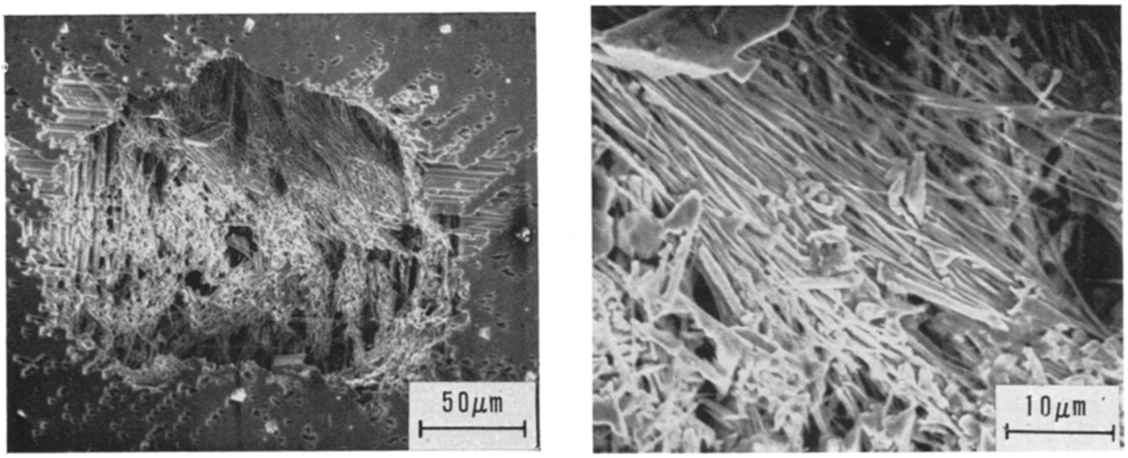

(a) (b)

Fig. 10. Scanning electron micrographs showing detailed structure of the deep pits formed by dissolution in the dark of sample A, area IV.